ELECTRONIC STRUCTURE AND CHEMICAL BOND NATURE IN $Cs_2NpO_2Cl_4$

by

Yury A. TETERIN [1,2*], ***Konstantin I. MASLAKOV*** [2], ***Mikhail V. RYZHKOV*** [3], ***Anton Yu. TETERIN*** [1], ***Kirill E. IVANOV*** [1], ***Stepan N. KALMYKOV*** [2], ***Vladimir G. PETROV*** [2], ***and Dmitry N. SUGLOBOV*** [4]

[1] NRC "Kurchatov Institute", Moscow, Russia
[2] Chemistry Department, Lomonosov Moscow State University, Moscow, Russia
[3] Institute of Solid State Chemistry, Ural Department of RAS, Ekaterinburg, Russia
[4] V.G. Khlopin Radium Institute, St.-Petersburg, Russia

Scientific paper
http://doi.org/10.2298/NTRP1701001T

On the basis of the X-ray photoelectron spectroscopy data and results of theoretical calculations for the $Np O_2Cl_4^{2-}$ (D_{4h}) cluster, the electronic structure and the chemical bond nature in $Cs_2NpO_2Cl_4$ single crystal, containing the neptunyl group NpO_2^{2+}, was done in the binding energy range of 0 eV to 35 eV. The filled Np 5f electronic states were established to form in the valence band of $Cs_2NpO_2Cl_4$. This was attributed to the direct participation of the Np 5f electrons in the chemical bonding. The Np 6p electrons were shown to participate in formation of both the inner valence band (15 eV- 35 eV) and the outer valence band (0 eV- 15 eV). The filled Np 6p and the O 2s, Cl 3s electronic shells were found to make the largest contribution to the formation of the inner valence molecular orbitals. The molecular orbitals composition and the sequence order in the binding energy range 0 eV- 35 eV in $Cs_2NpO_2Cl_4$, were established. For the first time the quantitative scheme of molecular orbitals for the $NpO_2Cl_4^{2-}$ cluster in the binding energy range 0 eV- 35 eV, was built. This scheme reflects neptunium close environment in the studied compound and is fundamental for both understanding the chemical bond nature in $Cs_2NpO_2Cl_4$ and the interpretation of other X-ray spectra of $Cs_2NpO_2Cl_4$. The contributions to the chemical binding for the $NpO_2Cl_4^{2-}$ cluster were evaluated to be: the outer valence molecular orbitals contribution – 73 %, and the inner valence molecular orbitals contribution – 27 %.

Key words: actinide, neptunium, electronic structure, XPS, relativistic calculation

INTRODUCTION

The valence X-ray photoelectron spectra (XPS) range of actinide compounds is especially important since it reflects the total density of states (DOS) of the valence electrons with photoionization cross-sections in mind [1-5]. However, interpretation of the valence XPS structure requires understanding of how effective (experimentally observable) a certain structure-formation effect appears in this binding energy (BE) range. It requires the studies of the core XPS spectra ~35 eV-1250 eV BE [5].

This paper presents the results of the quantitative analysis of the valence XPS structure (0~35 eV BE) of $Cs_2NpO_2Cl_4$ single crystal synthesized in [5]. For the first time the quantitative scheme of molecular orbitals (MO) was built, contributions of electrons of the outer (OVMO) and the inner (IVMO) valence molecular orbitals to the chemical binding were evaluated. The analysis was carried out taking into account the electron BE, core-outer electronic level BE differences and the core electron (~35 eV-1250 eV BE) XPS structure parameters measured in [5], as well as the novel relativistic calculation results for the $NpO_2Cl_4^{2-}$ (D_{4h}) cluster, reflecting neptunium close environment in $Cs_2NpO_2Cl_4$ at various interatomic distances.

CALCULATIONS

The electronic structure of the $NpO_2Cl_4^{2-}$ (D_{4h}) clusters was calculated in the density functional theory (DFT) approximation using the original code of the fully relativistic discrete variation (RDV) cluster method with exchange-correlation potential. The more detailed information can be found in [6].

In $Cs_2NpO_2Cl_4$ neptunium is surrounded by two oxygen ions in the axial directions (neptunyl group NpO_2^{2+}) and by four chlorine ions in the equatorial plane. The crystal structure parameters are: R_{Np-O} = = 0.1758(2) nm and R_{Np-Cl} = 0.2657(5) nm [3]; R_{Np-O} = = 0.1775(17) nm, and R_{Np-Cl} = 0.2653(3) nm [7]. In order to evaluate the influence of interatomic distances on the MO energies in the Cl 3s BE range, the elec-

* Corresponding authors; e-mail: teterin_ya@nrcki.ru

tronic structure calculations were done for the three clusters $NpO_2Cl_4^{2-}$ with interatomic distances: (a) $R_{Np-O} = 0.1710$ nm and $R_{Np-Cl} = 0.2620$ nm; (b) $R_{Np-O} =$ $= 0.1740$ nm and $R_{Np-Cl} = 0.2640$ nm; (c) $R_{Np-O} =$ 0.1760 nm and $R_{Np-Cl} = 0.2660$ nm. To evaluate the orbital forces, the calculations were done for: (a) $R_{Np-O} =$ $= 0.1758$ nm and $R_{Np-Cl} = 0.2657$ nm; (b) $R_{Np-O} =$ $= 0.1778$ nm, and $R_{Np-Cl} = 0.2657$ nm; (c) $R_{Np-O} =$ $= 0.1758$ nm, and $R_{Np-Cl} = 0.2677$ nm. For the case of the $NpO_2Cl_4^{2-}$ cluster, the re-normalization of the valence oxygen and chlorine atomic orbitals (AO) populations during the self-consistency, was done.

RESULTS AND DISCUSSION

XPS structure of CsCl and valence XPS structure of $Cs_2NpO2Cl_4$

The XPS structure of $Cs_2NpO_2Cl_4$ in the whole BE range of 0 eV-1250 eV is typical for this compound and corresponds to neptunium oxidation state Np(VI) ([5], tab. 1).

The basic peaks of CsCl XPS are intense and contain the many-body perturbation related structure at the higher BE side. This structure in the BE range 0-1250 eV was studied and discussed in details in [13]. It was established that in the core level Cs and Cl XPS spectra satellites appear. Intensity of such satellites drops in the low BE valence range. This structure was taken into account on interpretation of the $Cs_2NpO_2Cl_4$ valence XPS structure.

The experimental valence band XPS of $Cs_2NpO_2Cl_4$ exhibits a complicated structure, fig. 1(a). It can be suggested to consist of the XPS of the $NpO_2Cl_4^{2-}$ ion and two cesium Cs^+ ions. The valence XPS of the $NpO_2Cl_4^{2-}$ cluster is superimposed with the Cs $5s^25p^66s^0$ XPS of the two Cs^+ ions. Therefore, the CsCl XPS is given under the $Cs_2NpO_2Cl_4$ XPS, fig. 1(b).

The low BE CsCl XPS contains extra peaks at the higher BE side from the basic Cs 5s and Cs 5p peaks, attributed to the shake-up satellites and other energy loss spectra. These extra peaks complicate the interpretation of the $Cs_2NpO_2Cl_4$ XPS, although they can be taken into account. The contribution of this ex-

Table 1. Electron binding energies E_b [eV] and photo-ionization cross-sections σ at 1486.6 eV

Np *nlj* O *nlj*	$Cs_2NpO_2Cl_4$	$Cs_3NpO_2Cl_4$	NpO_2[a]	Np[b]	Np_{Theor}[e]	σ[d]
Np 5f	3.2(1.3)[e]	2.5	1.7 (1.3)	0.3	0.3	24.6
Np $6p_{3/2}$	16.1(2.1)	15.7	17.2 (3.1)		17.5	5.33
	20.0	18.6				
Np $6p_{1/2}$	30.1(3.0)	30.0	29.0(2.8)		29.1	1.81
Np 6s	50.2(6.8)	48.7(6.8)	46.7(5.5)		50.1	2.34
Np $5d_{5/2}$	102.4(2.1)	101.1(2.7)	100.4(4.1)		100.0	49.3
Np $5d_{3/2}$	112.1(3.3)	110.0(3.1)	108.9(9.5)		113.3	33.5
Np $5p_{3/2}$	208.7	207.3	201.5		213.7	31.4
			206.0			
Np $5p_{1/2}$			273(10)		273.6	9.22
Np 5s		335.2	337		342.2	10.2
			346			
Np $4f_{7/2}$	404.6(1.6)	403.4(1.6)	402.6(1.6)	400.1	401.3	396
Np $4f_{5/2}$	416.4(1.6)	415.2(1.6)	414.3(1.6)	411.8	413.8	310
Np $4d_{5/2}$	771.4(6.1)	770.3(4.3)	769.5(5.0)		772.5	238
Np $4d_{3/2}$	816.4	815.4	814.5(5.0)		817.8	156
Np $4p_{3/2}$	1087.4(8.4)	1086.1(7.4)	1084.8(13.6)		1089.5	108
O 2p	5.1	4.9	3.9(2.9)			0.27
			6.4(1.8)			1.91
O 2s	25.8	26.2	21.6			
O 1s	531.8(1.8)	531.6(1.8)	529.7(1.0)			40.0
Cs 6s						0.16
Cs $5p_{3/2}$	10.4(1.2)	10.4(1.2)	[10.1(1.2)][e]			4.52
Cs $5p_{1/2}$						2.31
Cs 5s	23.6(1.3)	23.5(1.3)	[23.4(1.4)]			2.50
Cl 3p			[4.4(1.4)]			2.35
Cl 3s	16.0(1.8)	15.7(1.8)	[15.0(1.2)]			2.52
Cl $2p_{3/2}$	198.6(1.2)	198.5(1.2)	[197.6(1.2)]			20.6

[a] NpO_2 values from [8]; [b] Values for metallic Np from [9, 10]; [c] Calculation data from [11], Values given relative to the Np5f peak from metallic Np; [d] Photoionozation cross-section σ (kilo barn ($10^{-25}m^2$) per atom) from [12]; and [e] FWHM are given in parentheses, values for CsCl are given in brackets. FWHM given relative Γ(C1s) = 1.3 eV

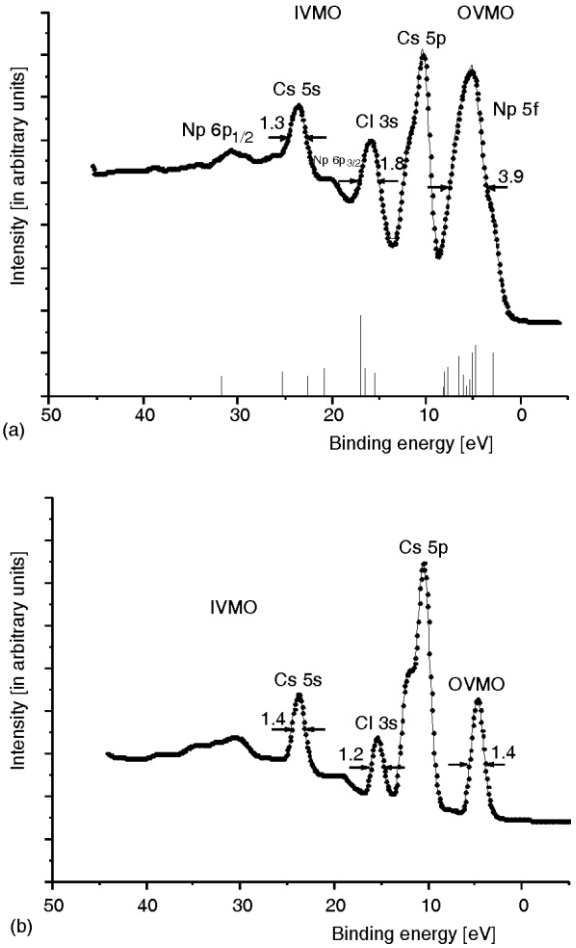

Figure 1. Valence band XPS: XPS from $Cs_2NpO_2Cl_4$ with the secondarily scattered electrons background. The vertical bars show the calculated (RDV) spectrum (a); XPS from CsCl with the subtracted secondarily scattered electrons background (b). Spectra normalized by the Cs 5p intensity

tra structure was taken into account on the basis of the analysis of the $Cs_2NpO_2Cl_4$ and CsCl satellite structure in the 0-1250 eV BE range. It has to be taken into account that the XPS from Cs^+ ion in $Cs_2NpO_2Cl_4$ can change compared to that from Cs^+ in CsCl.

To evaluate this contribution, the difference spectrum was drawn. It was obtained by subtraction of the Cs^+ XPS consisting of the Cs 5s, 5p peaks with satellites from the $Cs_2NpO_2Cl_4$ XPS without taking into account the background related to backscattering (fig. 2). Despite the approximation inaccuracy, the resulting spectrum agrees qualitatively with the calculated spectrum for the $NpO_2Cl_4^{2-}$ cluster, reflecting neptunium close environment in $Cs_2NpO_2Cl_4$.

To draw the difference spectrum, the XPS $Cs_2NpO_2Cl_4$ and CsCl intensities were normalized to the Cs 5p spin-orbit doublet (E_{sl}(Cs5p) = 1.6 eV) intensity. It has to be noted that on moving from CsCl to $Cs_2NpO_2Cl_4$, the Cs 5s and the Cs 5p peaks shift to the higher BE region by ~0.2 eV, and the Cl 3s peak – shifts by 1.0 eV (tab. 1). The difference spectrum was drawn for the two cases: (a) without subtraction of the

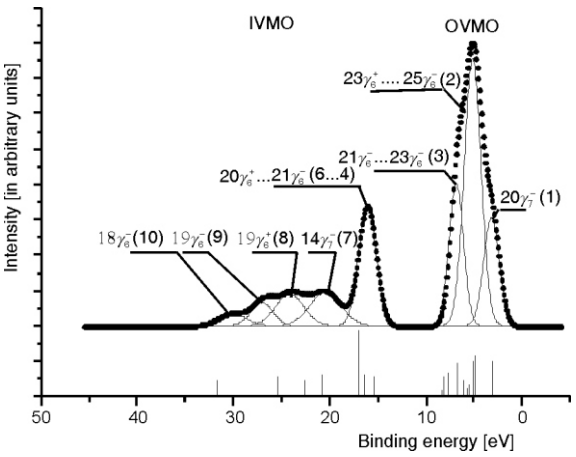

Figure 2. The difference of the valence XPS of $Cs_2NpO_2Cl_4$ and Cs^+ ions with the subtracted secondarily scattered electrons background (see fig. 1)

background related to secondary scattered electrons from the initial spectra; (b) with subtraction by Shirley [14] of the background related to secondary scattered electrons from the initial spectra (fig. 2). Despite the complicated structure, the difference spectra are in a good qualitative agreement.

The XPS structure in fig. 2 can be associated with formation of the OVMO (0-~15 eV) and IVMO (~15 eV-~35 eV) in the $NpO_2Cl_4^{2-}$ cluster (tab. 2). This structure has much in common with that of the $PuO_2Cl_4^{2-}$ structure discussed in details in [13]. The calculation results agree satisfactorily with the experimental data (tab. 3) and show that the Np 5f electrons participate in the chemical bond formation slightly losing their *f*-nature. The Np 6p electrons participate noticeably in both the OVMO and IVMO formation (tabs. 2 and 3).

Since photoemission results are given for an excited state of an atom with a hole in a certain shell, for a stricter comparison of the theoretical and experimental BE, the calculations must be done for transition states [15]. However, the work [13] showed that this effect results in a constant BE shift of the valence peaks, which was taken into account on comparison of the experimental and calculated spectra (tab. 3).

The experimental corroboration of the fact that the An 5f electrons maintain their *f*-nature during the chemical binding, *i. e*. participate directly and bring a high contribution to the valence DOS and XPS intensity, is fundamental. This allows using the MO LCAO (molecular orbitals as linear combinations of atomic orbitals) approximation for calculation of the XPS spectra with photoemission cross-sections in mind. This method neglects the nepheloauxetic effect (cloud expanding effect) for the 5f orbitals upon the chemical binding. Unfortunately, comparison of the experimental and calculated XPS spectra of $Cs_2NpO_2Cl_4$ yields a conclusion that the nepheloauxetic effect cannot be evaluated within the measurement error.

Table 2. MO compositions (parts) and energies E_0 [(a)] [eV] for the $NpO_2Cl_4^{-2}$ cluster (RDV) and photoionization cross-sections σ_i [(b)]

MO		$-E_0$ [eV]	MO composition													
			Np										O		Cl	
			6s	$6p_{1/2}$	$6p_{3/2}$	$6d_{3/2}$	$6d_{5/2}$	7s	$5f_{5/2}$	$5f_{7/2}$	$7p_{1/2}$	$7p_{3/2}$	2s	2p	3s	3p
			σ_i 1.16	0.90	1.32	0.62	0.56	0.12	4.12	3.86	0.06	0.08	0.96	0.07	1.26	0.47
OVMO	$28\gamma_6^+$	–14.86				0.28	0.48	0.09					0.07	0.06		0.02
	$31\gamma_6^-$	–8.07							0.02	0.02	0.90	0.01	0.01	0.01	0.01	0.02
	$22\gamma_7^+$	–7.80				0.05	0.76							0.05	0.02	0.12
	$21\gamma_7^+$	–7.42				0.34	0.46							0.12	0.01	0.07
	$30\gamma_6^-$	–7.42									0.01	0.96		0.01		0.02
	$24\gamma_7^-$	–7.30			0.01							0.95		0.02	0.01	0.01
	$27\gamma_6^+$	–7.29				0.45	0.32	0.02						0.17		0.04
	$26\gamma_6^+$	–6.60				0.03	0.01	0.77						0.02	0.04	0.13
	$29\gamma_6^-$	–5.60		0.01	0.07				0.12	0.34	0.03		0.02	0.40		0.01
	$20\gamma_7^+$	–4.35				0.42	0.42									0.16
	$23\gamma_7^-$	–2.29							0.09	0.66		0.01		0.21		0.03
	$28\gamma_6^-$	–1.91							0.42	0.30				0.21		0.07
	$27\gamma_6^-$	–1.14							0.04	0.82				0.04		0.10
	$22\gamma_7^-$	–0.89							0.04	0.88						0.08
	$21\gamma_7^-$	–0.26							0.74	0.08						0.18
	$20\gamma_7^{-(c)}$	0.00							0.79	0.15				0.02		0.04
	$25\gamma_6^+$	1.54														1.00
	$26\gamma_6^-$	1.71			0.03				0.03	0.02		0.01		0.07		0.84
	$19\gamma_7^+$	1.79					0.01							0.06		0.93
	$24\gamma_6^+$	1.80				0.01								0.06		0.93
	$19\gamma_7^-$	1.99			0.01				0.04	0.03		0.01		0.01		0.90
	$18\gamma_7^-$	2.08			0.01				0.02	0.03		0.01		0.02		0.91
	$25\gamma_6^-$	2.10								0.08	0.01					0.90
	$17\gamma_7^-$	2.15			0.01				0.19	0.01				0.01		0.78
	$24\gamma_6^-$	2.41			0.01				0.03	0.04	0.02			0.02	0.01	0.87
	$18\gamma_7^+$	2.75				0.07	0.09									0.84
	$17\gamma_7^+$	3.14				0.07	0.08								0.03	0.82
	$23\gamma_6^+$	3.18				0.01	0.01	0.06						0.06	0.02	0.84
	$23\gamma_6^-$	3.65		0.01	0.07				0.12	0.29	0.01	0.02		0.33		0.15
	$16\gamma_7^-$	4.78			0.02				0.09	0.17				0.70		0.02
	$22\gamma_6^+$	4.85	0.01			0.01	0.04	0.02					0.06	0.80	0.01	0.05
	$22\gamma_6^-$	5.05		0.01					0.21	0.05				0.73		
	$16\gamma_7^+$	5.26				0.05	0.15							0.77		0.03
	$21\gamma_6^+$	5.36				0.15	0.06							0.75		0.03
IVMO	$21\gamma_6^-$	12.41		0.01	0.32				0.01	0.01		0.01	0.44	0.10	0.10	
	$15\gamma_7^-$	13.41			0.11							0.01			0.87	
	$15\gamma_7^+$	14.04				0.01	0.03								0.94	0.02
	$20\gamma_6^-$	14.05		0.01	0.02					0.01	0.02		0.07		0.87	
	$20\gamma_6^+$	14.19				0.01	0.01	0.03							0.94	0.01
	$14\gamma_7^-$	17.22			0.84									0.02	0.11	0.02
	$19\gamma_6^+$	19.53	0.02			0.04	0.06						0.85	0.03		
	$19\gamma_6^-$	22.33		0.21	0.43					0.01			0.30	0.04	0.01	
	$18\gamma_6^-$	28.69		0.74	0.05								0.16	0.05		
	$18\gamma_6^+$	45.71	0.97										0.02	0.01		

[(a)] Levels shifted by 5.58 eV toward the positive values (upward); [(b)] Photo ionization cross-sections σ_i (kilo barn per electron), for O and Cl from [12]; [(c)] HOMO (highest occupied MO) (one electrons), occupation number for all the orbitals is 2

Results of tab. 1 on the experimental core-outer MO BE differences in both the $NpO_2Cl_4^{2-}$ cluster and metallic Np and the relativistic MO LCAO calculation data (fig. 3), allowed a quantitative MO scheme for the $NpO_2Cl_4^{2-}$ (D_{4h}) cluster (fig. 3). This scheme is important for understanding the chemical bond nature in the $NpO_2Cl_4^{2-}$ cluster.

For example, let's take the antibonding $21\gamma_6^-$(4) and $15\gamma_7^-$(5), the corresponding bonding $19\gamma_6^-$(9) and $14\gamma_7^-$(7) IVMO and the quasiatomic $15\gamma_7^+$, $20\gamma_6^-$, $20\gamma_6^+$(6), and $19\gamma_6^+$(8) ones attributed mostly to the Cl 3s and the O 2s electrons. The BE of the Cl 3s quasiatomic IVMO have to be close by an order of magnitude. We really see this in the XPS spectra as the Cl 3s peak of CsCl (E_b(Cl 3s) = 15.0 eV, Γ =1.2 eV). In $Cs_2NpO_2Cl_4$ XPS this is observed as a peak at E_b (Cl 3s) = 16.0 eV and Γ =1.8 eV (tab. 1). This peak is observed shifted and widened due to the Cl 3s electrons participation in the IVMO formation (fig. 1).

The BE of the quasiatomic $19\gamma_6^+$(8) IVMO should be about 23.8 eV since E_O = 508.0 eV and the O 1s BE in $Cs_2NpO_2Cl_4$ XPS is E_b(O 1s) = 531.8 eV

Table 3. Valence XPS parameters for $Cs_2NpO_2Cl_4$ and for the $NpO_2Cl_4^{2-}$ cluster (RDV), and the orbital forces[a] f_O and f_{Cl}, Np 6p and Np 5f electronic state density $\rho_i(e^-)$

MO		$-E$[b] [eV]	f_O 10^{-8} N	f_{Cl} 10^{-8} N	XPS Energy[c] [eV]	XPS Intensity [%]		Density $_i$ of the Np 6p,5f states in e^- (electrons)			
					Exper.	Theory	Exper.	$5f_{5/2}$	$5f_{7/2}$	$6p_{1/2}$	$6p_{3/2}$
OVMO	$20\gamma_7^-$[d]	3.30	–0.11*	–0.03*	3.2 (1.3)	8.0	12.8	0.79	0.15		
	$25\gamma_6^+$	4.54	–0.17	0.07		2.0					
	$26\gamma_6^-$	4.71	–0.17	0.04		2.7		0.06	0.04		0.06
	$19\gamma_7^+$	4.79	–0.13	0.07		1.9					
	$24\gamma_6^+$	4.80	–0.13	0.07		1.9					
	$19\gamma_7^-$	4.99	–0.18	0.09		3.0		0.08	0.06		0.02
	$18\gamma_7^-$	5.08	–0.18	0.07		2.7		0.04	0.06		0.02
	$25\gamma_6^-$	5.10	–0.18	0.10	5.1 (2.1)	3.0	34.0		0.16		
	$17\gamma_7^-$	5.15	–0.19	0.09		5.0		0.38	0.02		0.02
	$24\gamma_6^-$	5.41	–0.18	0.08		3.0		0.06	0.8		0.02
	$18\gamma_7^+$	5.75	–0.16	0.16		2.0					
	$17\gamma_7^+$	6.14	–0.19	0.09		2.1					
	$23\gamma_6^+$	6.18	–0.17	0.13		1.8					
	$23\gamma_6^-$	6.65	0.15	0.01	6.8 (1.7)	7.5	15.6	0.24	0.58	0.02	0.14
	$16\gamma_7^-$	7.78	0.56	–0.03		4.6		0.18	0.34		0.04
	$22\gamma_6^+$	7.85	0.36	–0.02		0.8					
	$22\gamma_6^-$	8.05	0.63	–0.04		4.6		0.42	0.10	0.02	
	$16\gamma_7^+$	8.26	0.62	–0.01		0.8					
	$21\gamma_6^+$	8.36	0.62	–0.01		0.8					
	$\Sigma\rho_1$[e]		0.80	0.93		58.2	62.4	3.04	1.74	0.04	0.32
			(61.5 %)	(78.8 %)							
IVMO	$21\gamma_6^-$	15.41	–0.43	–0.05		4.4		0.02	0.02	0.02	0.64
	$15\gamma_7^-$	16.41	–0.16	0.02	16.1(2.1)	5.2	15.9				0.22
	$15\gamma_7^+$	17.04	–0.18	0.13		5.0					
	$20\gamma_6^-$	17.05	–0.22	0.10		5.1		0.02	0.04	0.02	0.04
	$20\gamma_6^+$	17.19	–0.18	0.14		5.0					
	$14\gamma_7^-$	20.72	–0.08	0.08	20.4(3.7)	5.1	8.1				1.68
	$19\gamma_6^+$	22.53	0.53	–0.04	24.1(3.5)	3.7	6.9				
	$19\gamma_6^-$	25.33	0.47	–0.02	27.0(2.7)	4.6	3.9		0.02	0.42	0.86
	$18\gamma_6^-$	31.69	0.72	–0.05	30.1 (3.5)	3.7	2.8			1.48	0.10
	$\Sigma\rho_i$[f]					41.8	37.6	0.02	0.06	1.94	3.54
	$18\gamma_6^+$	48.71	0.03	–0.06	50.2 (7.4)	4.5					
	Σf[g]		0.50	0.25							
			(38.5 %)	(21.2 %)							
	Σf[h]		1.30	1.18							

[a] Orbital force newtons (N) per one ligand: f_O for Np-O bond and f_{Cl} for Np-Cl bond. Positive forces mean attraction, negative – repulsion; [b] Calculated energies (tab. 2) shifted by 3.00 eV toward the negative values (downward) so that the $20\gamma_7^-$ MO energy is 3.0 eV; [c] FWHM in eV given in parentheses; [d] HOMO (highest occupied MO) (1 electrons), occupation number for all the orbitals is 2; [e] The sum of the OVMO orbital forces peak intensities and the Np 6p, 5f DOS; [f] The sum of peak intensities and the Np 6p, 5f DOS, [g] The sum of the IVMO orbital forces; [h] The sum of the OVMO and IVMO orbital forces

(tab. 1). These data partially agree with the theoretical results.

Taking into account that the calculated E^t_{Np} = = 383.8 eV [11], and the difference E_1 = 389.2 eV, one can find that $_1$ = E_1 – E_{Np} is 5.2 eV (fig. 3). Since the BE difference between the $21\gamma_6^-(4)$ and $18\gamma_6^-(10)$ IVMO is 16.28 eV, and the Np 6p spin-orbit splitting, according to the calculation data [11], is E^{Theor}_{sl}(Np 6p) = 11.6 eV, one can evaluate that the perturbation $_1$ = 4.68 eV is some what lower than the corresponding value of 5.2 eV, found from the BE difference between the core and the valence MO. The observed difference must be attributed to the IVMO formation peculiarities and such a comparison may not be quite correct. The IVMO FWHM can not yield a conclusion on the IVMO nature (bonding or antibonding), however, one can suggest that the admixture of 10 % of the O 2p and 2 % of the Np 5f AO in the $21\gamma_6^-(4)$ IVMO leads this orbital to loosing of its antibonding nature (tab. 2, fig. 3). In the work [5] a similar scheme was shown to describe and explain the nature of chemical bond formation in γ-UO_3.

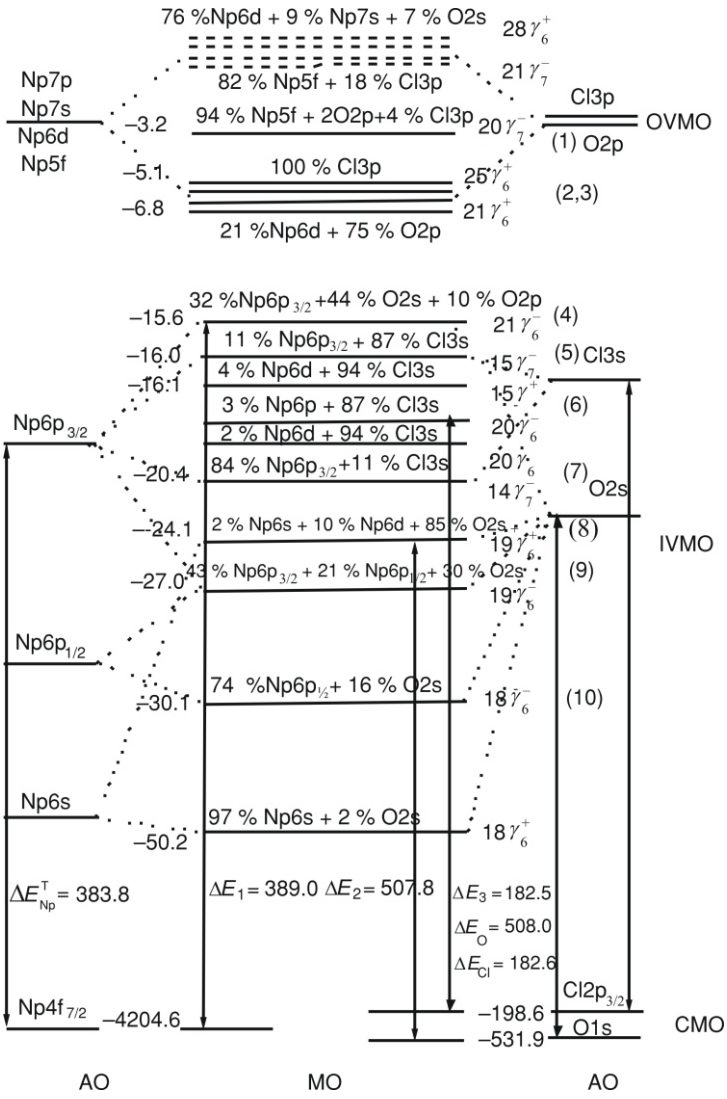

Figure 3. MO scheme for the $NpO_2Cl_4^{2-}$ (D_{4h}) cluster built taking into account theoretical and experimental data. Chemical shifts are not indicated. Arrows show some of the measured differences in BE between selected levels. Experimental BE (eV) are given to the left. The energy scale is omitted

Chemical bond in the $NpO_2Cl_4^{2-}$ cluster

Electronic configuration of neptunium ground state $^6L_{5\text{-}1/2}$ can be presented as [Rn] $6s^26p^65f\ ^46d^17s^27p^0$, where [Rn] is radon electronic configuration, and the other electronic shells are valence and can participate in the MO formation with the O $2s^22p^6$ and Cl $3s^23p^5$ AO in the $NpO_2Cl_4^{2-}$ cluster.

The RDV calculation results of the electronic structure of the $NpO_2Cl_4^{2-}$ (D_{4h}) cluster in the ground state, reflecting neptunium close environment in $Cs_2NpO_2Cl_4$, are given in tab. 2. The MO LCAO approximation, used in this calculation, allows discussion of the chemical bond nature in the terms of atomic and molecular shells.

The chemical bond formation and the AO overlapping, result in the OVMO and the IVMO formation. Beside the Np 6s,6p,5f,6d,7s, O 2s,2p, and Cl 3s,3p AO, these MO include the Np 7p states, which are absent in atomic neptunium. The RDV calculations show that the Np 6s AO, as well as the Np 7s and the Np 7p AO, participate insignificantly in the MO formation (tab. 2). While the Np 5f AO participate mostly in the OVMO formation, the Np 6p,6d AO participate in formation of both the OVMO and the IVMO. The largest Np $6p_{3/2}$ and the O 2s AO mixing of the neighboring neptunium and oxygen, was observed for the $21\gamma_6^-$ (4) and the $19\gamma_6^-$ (9) IVMO (tab. 2). The Np $6p_{1/2}$ – O 2s AO mixing in the $19\gamma_6^-$ (9) and the $18\gamma_6^-$ (10) IVMO is much higher than that in NpO_2 [8] because the interatomic distance $R_{Np\text{-}O}$ in the neptunyl group is lower than that in NpO_2. A significant mixing was observed only for the Np $6p_{3/2}$ and the Cl 3s AO, with formation of the $15\gamma_7^-$ (5) and the $14\gamma_7^-$ (7) IVMO.

The obtained results suggest subdividing the valence MO into three groups. The first group: $20\gamma_7^-$ (1) – $21\gamma_6^+$ (2, 3) OVMO. The second group: $21\gamma_6^-$(4), $19\gamma_6^+$ (8), $19\gamma_6^-$(9), $18\gamma_6^-$(10) and $18\gamma_6^+$ IVMO characterizing the Np-O binding in the axial direction. The

third group: from $15\gamma_7^-(5)$, $15\gamma_7^+$, $20\gamma_6^-$, $20\gamma_6^+(6)$ to $14\gamma_7^-(7)$ IVMO characterizing the Np-Cl binding in the equatorial plane (tab. 2). These results allow one to understand the valence XPS structure of $Cs_2NpO_2Cl_4$.

At the present time there is no method to evaluate quantitatively a contribution of certain separate MO into the chemical bond even for diatomic molecules. Several methods of evaluation of the MO character (bonding, non-bonding, antibonding) were considered in [16]: the first one – on the basis of population by Mulliken; the second one – on the basis of full energy separation with subtraction of resonance energy characterizing the covalence of the chemical bond; and the third one – on the basis of orbital forces.

The force [16] acting on an atom in the polyatomic system is equal to the opposite full energy gradient at the point of location. The gradient components are usually calculated as the ratio of the full energy alteration upon the displacement of an atom to the value of this displacement. The full energy is the sum of the orbital energies minus the energy of interelectronic interactions. Since the energy of interelectronic interaction depends on the sum of the orbital energies, the full energy can be considered to be proportional to the sum of the orbital energies with a coefficient less than 1. In this case, the force acting on an atom can be determined as a value proportional to the sum of the orbital forces.

The orbital forces f_i (10^{-8} N) approximately are equal to the derivatives of the MO energies $E_i^{'}$ (10^{-8} N) upon the interatomic distances [16]. Therefore, this work presents the dependence of the MO energies for the $NpO_2Cl_4^{2-}$ cluster on the interatomic distance in the axial direction $R_{Np\text{-}O}$ (z-axis) and in the equatorial plane $R_{Np\text{-}Cl}$.

To evaluate the orbital forces, in addition to the calculation for the equilibrium atomic positions ($R_{Np\text{-}O}$ = 0.1758 nm, $R_{Np\text{-}Cl}$ = 0.2657 nm), two more calculations were also done. One for $R_{Np\text{-}O}$ = 0.1778 nm and the invariable positions of chlorine ions, and another one – with equal positions of oxygen ions but with increased Np-Cl distance to the four chlorine ions $R_{Np\text{-}Cl}$ = 0.2677 nm. This yielded the orbital forces f_i (derivatives $E_i^{'}$ of the OVMO and IVMO energies E_i upon the interatomic distances $R_{Np\text{-}O}$ and $R_{Np\text{-}Cl}$) (tab. 3). As it follows from tab. 3 and the MO scheme (fig. 3), the $18\gamma_6^+$,$18\gamma_6^-$ (10), $19\gamma_6^-(9)$, $19\gamma_6^+(8)$, IVMO from this group bring a significant bonding contribution (1.75 10^{-8} N) to the Np-O binding and a slight antibonding contribution (–0.17 10^{-8} N) to the Np-Cl interaction. On the other hand, the IVMO of the other group from the $14\gamma_7^-(7)$ to the $15\gamma_7^-(5)$ containing the Cl 3s states bring a significant bonding contribution (0.47 10^{-8} N) to the Np-Cl interaction and an antibonding contribution (–0.82 10^{-8} N) to the Np-O binding. As it was expected, the bonding OVMO around the valence band bottom ($21\gamma_6^-$-$23\gamma_6^-$) contribute significantly (2.94 10^{-8} N) to the Np-O binding even despite the antibonding nature (–2.14 10^{-8} N) of the other OVMO of this group. The total OVMO contribution to the Np-O bond is 1.30 10^{-8} N. The total OVMO contribution to the U-Cl binding per one bond is 0.93 10^{-8} N, which is comparable to that for the Np-O bond. On the basis of these data, the relative IVMO contribution to the Np-O binding per one bond in the $NpO_2Cl_4^{2-}$ cluster was evaluated as 38.5 %, and that of the OVMO contribution – 61.5 %. The relative IVMO contribution to the Np-Cl binding is 21.2 %, that of the OVMO – 78.8 % (tab. 3).

The structures of irreducible representations of the double D_{4h} group allows comparisons of the Np 6d and the Np 5f AO participation in the chemical bond since the γ_6^+ and γ_7^+ orbitals contain the 6d states and do not contain the 5f states, while the γ_6^- and the γ_7^- MO – *vice versa*, contain the 5f states and do not contain the 6d states. Table 3 shows that among the six bonding MO in the bottom part of the OVMO valence band there are three orbitals of each type. The fractions of the 6d AO in the $21\gamma_6^+$, 16 γ_7^+, and $22\gamma_6^+$ MO are 0.21, 0.20, and 0.05, respectively, while the fractions of the 5f AO in the $22\gamma_6^-$, $16\gamma_7^-$, and $23\gamma_6^-$ MO are 0.26, 0.26, and 0.41, respectively (tab. 2). Despite the fact that the fraction of the 5f AO is greater than that of the 6d AO, their contributions are comparable, and the $23\gamma^-$ orbital shows the least orbital force (0.15 10^{-8} N) among the six considered bonding MO. Among the Np-Cl bond-related OVMO, the upper MO starting with the $23\gamma_6^+$ show the highest orbital forces. The bonding role of the 6d states in the Np-Cl binding is also slightly higher than that of the 5f states. These results agree with the values of the overlapping occupations for the corresponding orbitals found in the present work. These results also agree with the data on the covalent contribution of the uranyl group UO_2^{2+} with $R_{U\text{-}O}$ = 0.173 nm to the MO. For uranyl group the method of the full energy separation and X -DV determination of the resonance energy E^R(eV) showed that the IVMO electrons contribution to the covalent component of the chemical bond is 37 % of the total contribution of all the MO [16]. Despite the approximation used for the evaluation of these data was not perfect, one can conclude that the theoretical and experimental studies of chemical bond can not neglect the IVMO formation effect in actinide compounds. These results agree qualitatively with the data on $Cs_2UO_2Cl_4$ [6].

CONCLUSIONS

The valence XPS spectral structure of $Cs_2NpO_2Cl_4$ in the binding energy range 0-~ 35 eV was studied with the core electron XPS structure, BE differences between the core and the valence electronic levels and the relativistic calculation results of the electronic structure of the $NpO_2Cl_4^{2-}$ (D_{4h}) cluster in mind.

Comparison of the experimental and theoretical results yielded that the Np 5f (3.92 Np 5f e^-) electrons participate directly in the chemical binding in $Cs_2NpO_2Cl_4$ partially losing their *f*-nature. These electrons are delocalized mostly within the outer valence band. The weakly bound Np 5f electrons (0.94 Np 5f e^-) were shown to be localized at 3.2 eV BE.

The Np 6p atomic shell, in addition to the effective (experimentally measurable) participation in the IVMO formation, was found to participate noticeably (0.36 Np 6p e^-) in the filled OVMO formation. The largest part in the IVMO formation was established to be taken by the Np $6p_{1/2,3/2}$ and the O 2s AO, and to a lesser extent – by the Np $6p_{3/2}$ and the Cl 3s AO of the neighboring neptunium, oxygen, and chlorine ions.

The MO sequent order in the BE range of 0-~35 eV for the $NpO_2Cl_4^{2-}$ cluster was defined and the corresponding MO composition was calculated. A fundamental quantitative MO scheme was built, which is important for understanding the nature of interatomic bonding in $NpO_2Cl_4^{2-}$ and for the interpretation of other X-ray spectra. The OVMO and IVMO contributions to the chemical bond were evaluated for the $NpO_2Cl_4^{2-}$ cluster. The relative OVMO contribution to the chemical binding was shown to be 73 %, and that of the IVMO – 27 %. This agrees with the results for $Cs_2UO_2Cl_4$ [6]. In conclusion we'd like to note that the theoretical and experimental studies of chemical bond cannot neglect the IVMO formation effect in actinide compounds.

ACKOWLEDGEMENTS

The work was supported by the RFBR grant No. 17-03-00277-a.

AUTHORS' CONTRIBUTIONS

The idea for the study was put forward by Y. A. Teterin, the measurements were carried out by K. I. Maslakov, the theoretical calculations were carried out by M. V. Ryzhkov, the compounds were produced by D. N. Suglobov, the samples were prepared by V. G. Petrov, and the experimental data were processed and interpreted by S. N. Kalmykov, A. Yu. Teterin and, K. E. Ivanov.

REFERENCES

[1] Veal, B.W., *et al*., X-Ray Photoelectron Spectroscopy Study of Oxides of the Transuranium Elements Np, Pu, Am, Cm, Bk and Cf, *Phys. Rev. B, 15* (1977), March, pp. 2929-2942
[2] Atuchin, V. V., Zhang, Z., Chemical Bonding Between Uranium and Oxygen in U^{6+}-Containing Compounds, *J. Nucl. Mater., 420* (2012), Jan., pp. 222-225
[3] Denning, R. G., Electronic Structure and Bonding in actinyl Ions, *Structure and Bonding, 79* (1992), pp. 215-276
[4] Denning, R. G., Electronic Structure and Bonding in actinyl Ions and their Analogs, *J. Chem. Phys., A 111* (2007), 20, pp. 4125-4143
[5] Teterin, Yu. A., Teterin, A. Yu., Structure of X-Ray Photoelectron Spectra of Light Actinide Compounds, *Russian Chemical Reviews, 73* (2004), 6, pp. 541-580
[6] Teterin, Yu. A., *et al*., Valence XPS Structure and Chemical Bond in $Cs_2UO_2Cl_4$, *Nucl Technol Radiat, 31* (2016), 1, pp. 37-50
[7] Wilkerson, M. P., *et al*., Crystal Structure and spectros-Copic Measurements of Room Temperature Intra-5f Fluorescence of $Cs_2Np(VI)O_2Cl_4$, *J. of Alloys and Compounds, 444-445* (2007), Oct., pp. 634-639
[8] Teterin, Y. A., *et al*., X-Ray Photoelectron Spectra Structure and Chemical Bond Nature in NpO_2, *Phys. Rev. B, 89* (2014), Jan., 035102
[9] Seibert, A., *et al*., Reaction of Neptunium with Molecular and Atomic Oxygen: Formation and Stability of Oxides, *Nucl. Mater., 389* (2009), 3, pp. 470-478
[10] Naegele, J. R., *et al*., Photoelectron Spectroscopy (UPS/XPS) Study of Np_2O_3 Formation on the Surface of Neptunium Metal, *Inorg. Chim. Acta., 139* (1987), 1-2, pp. 327-329
[11] Huang, K. N., *et al*., Neutral-Atom Electron Binding Energy from Relaxed-Orbital Relativistic Hartree-Fock-Slater Calculations, *At. Data Nucl. Data Tables, 18* (1976), 3, pp. 243-291
[12] Band, M., *et al*., Photoionization Cross Sections and Photoelectron Angular Distribution for X-Ray Line Energies in the Range 0.132-4.509 keV (Targets: 100 Z 1), *At. Data Nucl. Data Tables, 23* (1979), 5, pp. 443-505
[13] Teterin, Yu. A., *et al*., Electronic Structure and Chemical Bond Nature in $Cs_2PuO_2Cl_4$, *Nucl Technol Radiat, 30* (2015), 2, pp. 99-113
[14] Shirley, D. A., High-Resolution X-Ray Photoemission Spectrum of the Valence Band of Gold, *Phys. Rev. B, 5* (1972), pp. 4709-4714
[15] Slater, J. C., Johnson, K. H., Self-Consist Field X Cluster Method for Polyatomic Mole-Cules and Solids, *Phys. Rev. B, 5* (1972), 3, pp. 844-853
[16] Teterin, Yu. A., Gagarin, S. G., Inner Valence Molecular Orbitals and the Structure of X-Ray Photoelectron Spectra, *Russian Chemical Reviews, 65* (1996), 10, pp. 825-847

Received on October 24, 2016
Accepted on January 17, 2017

Јурий А. ТЕТЕРИН, Константин И. МАСЛАКОВ, Михаил В. РИШКОВ, Антон Ј. ТЕТЕРИН, Кирил Е. ИВАНОВ, Степан Н. КАЛМИКОВ, Владимир Г. ПЕТРОВ, Дмитриј Н. СУГЛОБОВ

ЕЛЕКТРОНСКА СТРУКТУРА И ПРИРОДА ХЕМИЈСКИХ ВЕЗА У $Cs_2NpO_2Cl_4$

На основу података рендгенске фотоелектронске спектроскопије и резултата теоријских прорачуна $N_pO_2Cl_4^{2-}$ (D_{4h}) кластера, одређена је електронска структура и природа хемијске везе у монокристалу $Cs_2NpO_2Cl_4$ који садржи нептунил групу NpO_2^{2+}, у опсегу енергије везе 0- 35 eV. Унета NP 5f електронска стања образовала су се у валентној зони $Cs_2NpO_2Cl_4$ и ово је приписано директном учешћу NP 5f електрона у хемијској вези. Показано је да Np 6p електрони учествују у формирању како унутрашње валентне зоне (15- 35 eV) тако и спољашње валентне зоне (0- 15 eV). Установљено је да унете Np 6p и O 2s, Cl 3s електронске орбите највише доприносе формирању молекуларних унутрашњих валентних зона. Одређени су композиција и секвенцијални поредак молекулских орбита у области енергија веза од 0- 35 eV у $Cs_2NpO_2Cl_4$ и по први пут квантификована шема молекулских орбита $NpO_2Cl_4^{2-}$ кластера у опсегу енергија везе 0- 35 eV. Ова шема одсликава непосредну околину нептунијума у проучаваном једињењу и основа је за разумевање природе хемијских веза у $Cs_2NpO_2Cl_4$, као и тумачење осталих рендгенских спектара $Cs_2NpO_2Cl_4$. Процењени су доприноси хемијском везивању $NpO_2Cl_4^{2-}$ кластера: спољашњим молекуларним валентним орбитама – 73 %, а унутрашњим молекуларним валентним орбитама – 27 %.

Кључне речи: актинид, нептунијум, електронска структура, рендгенска фотоелектронска спектроскопија, релативистички прорачун